Quantitative Assessment of Scots Pine (*Pinus Sylvestris* L.) Whorl Structure in a Forest Environment Using Terrestrial Laser Scanning

Jiri Pyörälä, Xinlian Liang, *Member, IEEE*, Mikko Vastaranta, Ninni Saarinen, Ville Kankare, Yunsheng Wang, *Member, IEEE*, Markus Holopainen, and Juha Hyyppä

***Abstract*—State-of-the-art technology available at sawmills enables measurements of whorl numbers and the maximum branch diameter for individual logs, but such information is currently unavailable at the wood procurement planning phase. The first step toward more detailed evaluation of standing timber is to introduce a method that produces similar wood quality indicators in standing forests as those currently used in sawmills. Our aim was to develop a quantitative method to detect and model branches from terrestrial laser scanning (TLS) point clouds data of trees in a forest environment. The test data were obtained from 158 Scots pines (*Pinus sylvestris* L.) in six mature forest stands. The method was evaluated for the accuracy of the following branch parameters: Number of whorls per tree and for every whorl, the maximum branch diameter and the branch insertion angle associated with it. The analysis concentrated on log-sections (stem diameter $>$15 cm) where the branches most affect wood's value added. The quantitative whorl detection method had an accuracy of 69.9% and a 1.9% false positive rate. The estimates of the maximum branch diameters and the corresponding insertion angles for each whorl were underestimated by 0.34 cm (11.1%) and 0.67° (1.0%), with a root-mean-squared error of 1.42 cm (46.0%) and 17.2° (26.3%), respectively. Distance from the scanner, occlusion, and wind were the main external factors that affect the method's functionality. Thus, the completeness and point density of the data should be addressed when applying TLS point cloud based tree models to assess branch parameters.**

***Index Terms*—Branch, forestry, LiDAR, modeling, wood procurement, wood quality.**

I. Introduction

THE wood quality of sawn goods determines the price acquired for the sawn goods and the allowable costs of production [1]. Wood quality is closely and inversely related to knots in the wood, because knots have a direct adverse effect on wood performance. For example, knots in sawn wood distort the stem wood grain orientation, and decrease wood stiffness and strength [2]. The numbers and the maximum knot size on a piece of sawn wood are the two of the knot parameters that are most often included in the grading of sawn goods [3], [4]. The projection size of a knot's cross section on a sawn board and its effect on a board's quality is dependent on both the diameter and the angle in which the knot emerges from the pith [5]. Knots are derived from branches, and log-specific branch parameters such as the maximum branch diameter can be used as a part of wood quality estimation and sawing optimization at sawmills [4], [6]. Three-dimensional (3-D) imaging or X-ray scanning can be used to assess the required branch and knot information on logs, namely the number of whorls and the maximum branch or knot size per whorl [7], [8]. However, sawmills plan their sawn wood production prior to the harvesting of trees. Missing information about wood quality of standing timber introduces uncertainty into the planning, and can lead to additional costs [9]. Foreknowledge of trees' branch parameters would be valuable for the sawing industry.

Terrestrial laser scanning (TLS) is a technology that can provide a high detail 3-D point cloud of environment and it can be used to measure wood quality indicators such as stem curve and branch parameters on standing trees. A multiscan TLS survey is usually performed from a few fixed positions, which limits the data coverage [10]–[12]. However, there are at least two approaches that can be used to overcome the spatial limitations.

Manuscript received November 9, 2017; revised February 1, 2018; accepted March 14, 2018. Date of publication April 18, 2018; date of current version October 15, 2018. This work was supported in part by the Finnish Academy projects "Centre of Excellence in Laser Scanning Research (CoE-LaSR) under Grant 272195", in part by "Interaction of Lidar/Radar Beams with Forests Using Mini-UAV and Mobile Forest Tomography" under Grant 259348, in part by "Competence Based Growth Through Integrated Disruptive Technologies of 3-D Digitalization, Robotics, Geospatial Information and Image Processing/Computing Point Cloud Ecosystem" under Grant 293389, in part by the European Community's Seventh Framework Programme (FP7/2007–2013) under Grant 606971, in part by the Ministry of Agriculture and Forestry of Finland project "Puuston laatutunnukset" (OH300-S42100-03), in part by the Foundation for Research of Natural Resources in Finland (1780/15, 1790/16, and 1798/17), in part by the Finnish Forest Foundation (2014092904), and in part by the Jenny ja Antti Wihurin rahasto. *(Corresponding author: Jiri Pyörälä.)*

J. Pyörälä is with the Department of Remote Sensing and Photogrammetry and the Centre of Excellence in Laser Scanning Research, Finnish Geospatial Research Institute, Masala FI-02431, Finland, and also with the Department of Forest Sciences, University of Helsinki, Helsinki FI-00014, Finland (e-mail: jiri.pyorala@nls.fi).

X. Liang, Y. Wang, and J. Hyyppä are with the Department of Remote Sensing and Photogrammetry, and the Centre of Excellence in Laser Scanning Research, Finnish Geospatial Research Institute, Masala FI-02431, Finland (e-mail: xinlian.liang@nls.fi; yunsheng.wang@nls.fi; juha.hyyppa@nls.fi).

M. Vastaranta is with the Department of Forest Sciences, University of Helsinki, Helsinki FI-00014, Finland, with the Centre of Excellence in Laser Scanning Research, Finnish Geospatial Research Institute, Masala FI-02431, Finland, and also with the School of Forest Sciences, University of Eastern Finland, Joensuu FI-80101, Finland (e-mail: mikko.vastaranta@helsinki.fi).

N. Saarinen, V. Kankare, and M. Holopainen are with the Department of Forest Sciences, University of Helsinki, Helsinki FI-00014, Finland, and with the Centre of Excellence in Laser Scanning Research, Finnish Geospatial Research Institute, Masala FI-02431, Finland (e-mail: ninni.saarinen@helsinki.fi; ville.kankare@helsinki.fi; markus.holopainen@helsinki.fi).

Digital Object Identifier 10.1109/JSTARS.2018.2819598

First, the current preharvest information is collected with the use of remote sensing. The sample plot data required for building predicative models could be obtained using TLS, adding the wood quality indicators to the suite of predicted inventory attributes of a stand [13], [14]. Second, instead of static TLS, detailed point clouds could be collected using a laser scanner mounted on a moving platform, i.e., mobile laser scanning (MLS) such as on a harvester [15].

The quantitative measurement of branch parameters using TLS entails a tree model at level of details (LoD) 3. The LoD 3 model includes stem and main branching structure, i.e., the branch bases diverting from the stem must be reconstructed [10]. Modeling of individual tree at LoD 3 and beyond, including full branches with twigs, has been demonstrated in previous studies, e.g., Cheng *et al*. [16], Gorte and Pfeifer [17], Bucksch and Lindenbergh [18], Côté *et al*. [19] and Raumonen *et al*. [20], to name just a few examples that represent different modeling approaches. Cheng *et al*. [16] segmented sparse TLS range images into patches and extracted the tree skeleton by analyzing the connections between the patches. Each patch was then modeled as a cylinder. The study by Gorte and Pfeifer [17] used a point cloud of a tree that was collapsed into voxels. Gorte and Pfeifer [17] removed the empty voxels, and the remaining voxels were reduced into a tree skeleton that was segmented into stem and branches based on the internode neighborhood-relations. In the study by Bucksch and Lindenbergh [18], a point cloud was divided into an octree to extract the skeleton. Côté *et al*. [19] combined a skeleton extraction method and a branch growth model to produce realistic tree models despite the data gaps in the point cloud. Raumonen *et al*. [20] on the other hand, used a quantitative structure model (QSM) approach that divided the point cloud into small spherical subsets of points. The subsets were characterized by their eigenvectors, and further skeletonized into a hierarchical structure that included tree trunk, branches, and twigs. The point cloud was then segmented using the skeletonized structure and each segment was modeled using a cylinder fitting. For further reading, at least Boudon *et al*. [21] and Bournez *et al*. [22] have carried out comparative studies between existing tree modeling methods that include individual branching parameters.

There has been a lack of studies that evaluate tree-modeling at LoD 3 in a forest environment. Raumonen *et al*. [23] showed that the QSM approach can be applied to forest plot conditions, too, but the group did not report how occlusion, wind, or other factors related to a forest environment affected the results. Côté *et al*. [24] scanned six trees in a forest environment and reported that also in the presence of occlusion and wind, the combined use of TLS point cloud processing and branch growth models reconstructed tree models with realistic branch distributions, when compared to destructive field measurements. In addition, only a few studies have tested branch measurements in forested conditions using semiautomatic methods, e.g., [25], [26]. In the first study, Dassot *et al*. [25] scanned 42 trees in a forest environment. The stems and branches with diameters exceeding 7 cm were then manually selected from the point clouds and modeled using automated cylinder fitting. In the second study, Eysn *et al*. [26] reconstructed comprehensive tree models semiautomatically utilizing the 2-D intensity maps of the point clouds comprising a 0.65 ha stand of old forest. Bayer *et al*. [27] skeletonized manually 42 tree point clouds in a mixed forest environment. All three groups reported that their method's accuracy was affected by the occlusion toward the tree top and the effect of wind.

TABLE I
PLOT INFORMATION

	Location	Site type	V_{Pine} (m^3*ha^{-1})	V_{other} (m^3*ha^{-1})
Plot 1	Evo	VT	220	10
Plot 2	Evo	VT	250	20
Plot 3	Evo	OMT	200	20
Plot 4	Evo	MT	140	260
Plot 5	Orimattila	MT	80	170
Plot 6	Orimattila	VT	170	80

VT = *Vaccinium* type, MT = *Myrtillus* type, OMT = *Oxalis-Myrtillys* type. V_{Pine} is the volume of pine and V_{other} is the volume of other species per hectare.

However, the accuracy in the acquisition of individual branch parameters that would be required for wood quality estimations in standing trees has not yet been comprehensively evaluated. A method for stem recognition and modeling reported by Liang *et al*. [28] was presented for TLS point clouds. The method used in this present study was broadened to include the main branching structure of trees. It was applied to multiscan point clouds of individual Scots pine (*Pinus sylvestris* L.) trees that were selected from varying forest conditions in order to capture and recognize the external factors that affect the method's functionality. The analyses concentrated on the log sections (i.e., part of a stem with diameter $>$15 cm), and the method was evaluated using branch parameters currently available in the sawmilling industry: The number of whorls and the maximum branch diameter and the insertion angle of the corresponding branch of each whorl. The evaluation was done by comparing the results of the TLS against visually identified whorls and manually measured branch parameters of the largest branch in each whorl. In addition, tree- and plot-specific factors affecting the method's functionality were analyzed. Thus, the aim of this study was to introduce a TLS point cloud based method that could be used on single trees *in situ* to detect branches and model their diameters and insertion angles, i.e., to produce similar branch parameters as produced by state-of-the-art wood quality estimation systems currently used at sawmills.

II. MATERIALS

A. Field Data

The study subject material consisted of data obtained from 158 Scots pines in six mature forest plots in southern Finland, i.e., four plots in Evo (61.19 °N, 25.11 °E) and two plots in Orimattila (60.80 °N, E 25.73 °E). The plots were mainly Scots pine- dominated, except for plots 4 and 5 that were mixed Scots pine and Norway spruce (*Picea abies* H. Karst.) forest. The sample plot forest inventory attributes are based on existing stand forest inventory data for the year 2013, as presented in Table I. The sample trees were selected in groups of three–six trees. The sample tree information is presented in Table II. Sample tree diameter at breast height (1.3 m, *DBH*) was measured by calipers. Tree height (*H*) and the heights of the lowest dead branch (H_{db}) and the live crown base (H_{lc}) were measured using the

TABLE II
SAMPLE TREE INFORMATION

		DBH (cm)		*H* (m)		H_{db} (m)		H_{lc} (m)	
	Trees	Mean	± SD	Mean	± SD	Mean	± SD	Mean	± SD
Plot 1	30	28.9	3.4	22.6	1.2	4.8	2	14.4	1.7
Plot 2	20	32.8	2.5	27	1.5	8.7	1.5	17.1	1.8
Plot 3	30	28.6	4.2	22.9	1.8	4.4	2.3	13.9	1.9
Plot 4	24	35.8	5	29	1.4	8.5	1.6	20.9	1.8
Plot 5	28	34.7	4.2	27.7	1.8	10	2.9	18.8	1.6
Plot 6	26	32.1	6	26	2.4	7.6	2.2	15.4	1.7
Total	158	31.8	5.2	25.5	3	7	3.1	16.6	3.0

Vertex III (Haglöf, Sweden). The data were collected in August 2014.

B. TLS Data Acquisition

TLS data were collected in the August–September period in 2014 using a Faro Focus^{3D} X 330 phase-shift scanner (Faro, USA). Each tree group was scanned from 5 to 10 positions. The number of scanning positions was dependent on the visibility in the plot and the scanning positions were distributed such that data coverage on all sides of all targeted trees was obtained. The mean horizontal distance between a scanning position and a tree was 9.6 m (see Table III). Six spheres were used as reference targets for coregistering the scans. The spheres were distributed to enable all six spheres to be visible in one of the scans and at least three spheres were visible in all the other scans. The sampling distance between two points with these scanner settings was 6.3 mm at 10 m distance. The mean point density was 17889pts/m^2 at H_{db}, which was based on the 3-D distance between the scanner and the lowest dead branch and the aforementioned point-to-point sampling distance: First, we calculated the point-to-point sampling distance at H_{db} by dividing the aforementioned point-to-point sampling distance (6.3 mm) by 10 m, and multiplying the result by the 3-D distance between the scanner and the lowest dead branch. Then, we calculated how many points fit in a square-meter given the point-to-point distance (see Table III).

Preprocessing of the TLS point clouds was carried out using Faro Scene software (version 5.2.1). Individual scans were coregistered, and dark and stray points were filtered out from the point clouds. The overall mean registration error of the reference target coordinates between the scans was 1.3 mm (see Table III).

Wind is known to have an effect on the quality of TLS data [29]. The mean and maximum wind speeds (m/s) during each plot scanning, as recorded by the nearest weather station of Finnish Meteorological Institute, are given in Table III.

III. METHODS

A. Manual Reference Measurements of the Branch Parameters Using the Point Clouds

Manual TLS point cloud measurements on the sample trees were carried out using TerraScan software (TerraSolid, Finland). Since the scope of this study was to evaluate a quantitative branch detection and modeling method, we avoided other processing steps that could have affected the results, including tree segmentation and extraction methods that are separate issues. Therefore, the sample trees were extracted from the point cloud manually. The extraction included removing the ground points, the stems, and the crowns of the surrounding trees. After extraction, each whorl's largest branch was identified visually. The points belonging to the visually identified largest branch in each whorl were extracted and the branch diameter was estimated by the means of manual circle fitting. The MicroStation's "Draw circle"–tool was used to place a circle around the extracted points perpendicularly to the longitudinal axis of the branch (see Fig. 1). The method did not account for stochastic noise or elliptical branch shape: The circle was drawn around all points that appeared to belong to the branch. Branch diameter (b_d) was given by the circle diameter. The height of the branch was defined as the difference between the circle center (b_c) *z*-coordinate and the visually estimated root collar height. Branch insertion angle b_α was defined as the angle between a vertical *Z*-axis $n_z = [0, 0, 1]$ and the normal $e_0 = [e_1, e_2, e_3]$ of the fitted circle similar to that described in the literature [5] (1). Descriptive statistics of the manual measurements are presented in Table IV

$$\cos b_\propto = n_z \cdot e_0. \tag{1}$$

B. Quantitative Whorl Detection Method

The extracted trees were modeled quantitatively by identifying points belonging to tree stems and fitting cylinders to them using a weighted least-squares optimization to minimize the distance of the points to the cylinder surface. Details of the method can be found in Liang *et al*. [28].

Points within 50-cm distance from the modeled stem surface were selected and divided into segments of 15 cm in height, in 5-cm intervals, i.e., consecutive segments had a vertical overlap of 10 cm. Each segment was analyzed for the distribution of point density and the mean distance of points from the stem over a 360° rotation around the stem, as shown in Fig. 2. Two distributions instead of one were used to separate branch points from interfering noise points, such as from branch bumps or other stem deformations that should not have a peak in the mean distance histogram, as shown in Fig. 2.

To smooth these data, the point density and mean distance distributions were convolved with a Gaussian window function using the Fourier transform [30]. Fourier transform converts the original data X_n in the spatial domain into X_k in the frequency domain by computing a discrete Fourier transformation

$$X_k = \sum_{n=0}^{N-1} x_n e^{-i2\pi kn/N} \tag{2}$$

where *N* is the periodic sequence of the data (360° around the stem in this case) and x_n is the function's value at *n* degrees. The complex sinusoidal component $e^{-i2\pi kn/N}$ determines the functions' amplitude and frequency, where *i* stands for the imaginary unit $\sqrt{-1}$. X_k is multiplied with the Gaussian window function, and transformed back to the original domain. The result is a convolution of the original function and the Gaussian window function. (see Fig. 2(c) and (d)) The standard deviation (σ) of the Gaussian distribution has an effect on the smoothing results, as it affects the width of peaks in the resulting convolution. In

TABLE III
TLS DATA COLLECTION STATISTICS

	Scanner-to-tree distance (m)		Point density at H_{db} (1000 pts/m^2)		Registration error (mm)		Wind speed (m/s)	
	Mean	± SD	Mean	± SD	Mean	± SD	Mean	Max
Plot 1	8.9	1.3	24.6	7.4	1.2	0.9	3.9	4.8
Plot 2	11.0	1.1	12.5	2.6	1.0	0.5	3.9	5.0
Plot 3	9.4	1.3	22.2	4.1	0.7	0.3	3.0	5.0
Plot 4	9.4	2.3	14.8	4.9	1.5	1.0	3.5	5.2
Plot 5	9.1	2.2	13.4	4.4	1.4	0.6	0.6	1.9
Plot 6	10.6	1.9	14.6	4.1	1.7	0.8	2.3	3.1
Mean	9.6	1.9	17.9	6.9	1.3	0.8	3.9	4.8

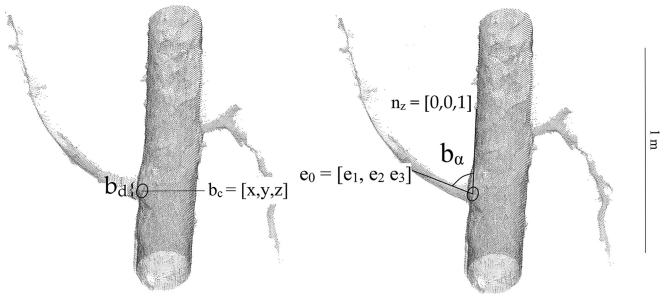

Fig. 1. Definition of the branch parameters used in this study: Branch diameter b_d, 3-D-location of a branch b_c and branch insertion angle b_α, i.e., the angle between the vertical z-axis n_z and the branch axis or eigenvector e_0.

TABLE IV
MANUAL BRANCH PARAMETER REFERENCE DATA STATISTICS

	Min	Mean	Max	± SD
Number of whorls	0	21.54	51	8.37
Lowest whorl (m)	0.83	7.04	13.50	2.66
Highest whorl (m)	9.23	15.69	21.47	2.36
Minimum branch diameter (cm)	0.86	1.65	3.01	0.40
Mean branch diameter (cm)	1.78	3.05	4.96	0.59
Maximum branch diameter (cm)	2.59	4.96	9.95	1.33
Minimum branch insertion angle (°)	6.69	41.48	67.58	10.13
Mean branch insertion angle (°)	46.91	64.98	80.58	6.44
Maximum branch insertion angle (°)	61.12	97.06	165.50	20.60

The number of whorls was 3403 and the number of trees 158.

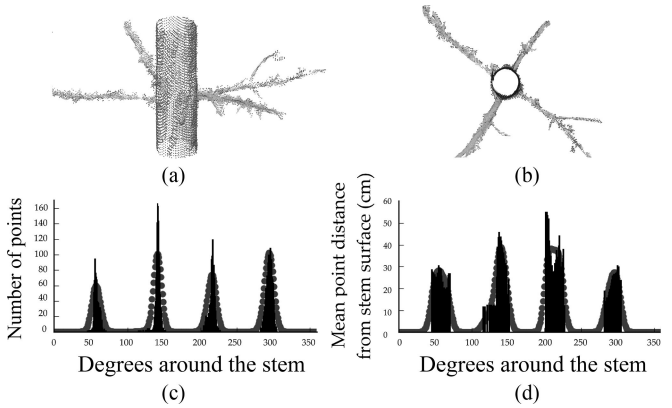

Fig. 2. Principle of branch detection. A whorl of four branches as seen from (a) side and (b) top view. (c) Number of points per degrees around the stem at the height of the whorl. (d) Mean distance of points from the stem surface per degrees around the stem. The gray line in (c) and (d) represents the convolution of a Gaussian window function and the original distribution that is used for peak detection.

this study, σ was set to 5, based on the testing of the parameters for two Scots pines that were not included in this study.

The resulting functions of point density and distance were then analyzed utilizing the continuous wavelet transform method (CWT) [31]. CWT is a robust signal-processing method where a continuous wavelet is scaled and transformed into the original function's domain and iteratively compared to the original function to find matching patterns. The result is a 2-D-array C_{wp} of wavelet coefficients that, intuitively, reflect the goodness of a pattern matching between the original function and the wavelet

$$C_{wp} = \frac{1}{\sqrt{w}} \int_{\infty}^{-\infty} c\,(t)\,\psi\left(\frac{t-p}{w}\right) dt \qquad (3)$$

where *c(t)* is the original function and $\psi(t)$ is a continuous wavelet, with *w* being the wavelet width or a scaling parameter, and *p* the position of the wavelet or a translation parameter. The wavelet $\psi(t)$ used in this study had a predefined width set ranging from 5° to 45° for the point density function and from 20° to 75° for the mean distance function, based on the testing of the parameters for two Scots pines that were not included in this study. The peak locations were identified as positions of local maxima in C_{wp}. The positions that exhibited peaks that satisfied the aforementioned conditions in both distributions were defined as branch positions. Points falling within each peak were labeled to belong to a single branch.

C. Branch Modeling Method

The points within a 2- to 12-cm distance from the stem that belong to an identified branch were projected onto a 2-D plane perpendicular to the branch's longitudinal axis and modeled as a circle using the RANSAC algorithm [32]. A local coordinate system was established for the branch points and the longitudinal axis direction was indicated by the eigenvector that corresponded to the largest eigenvalue.

In RANSAC algorithm, the solution of a model is sought iteratively. On each iteration round a random sample of three points was selected to which a circle was initially fitted using ordinary least squares approximation. Then, the ratio of points lying within a 0.5-mm distance from the circle arc (inliers) was calculated. The diameter of the circle fitted to the inliers from the iteration round that had the highest number of inliers was considered as the branch diameter estimate.

The branch insertion angle was calculated using the longitudinal axis direction (1). Branches that had near vertical insertion angles were filtered out of the data, such that $10^\circ < b_\alpha < 170^\circ$

in the data. This was done to exclude any further possible false positive detections caused by stem deformations and stochastic noise.

D. Evaluation of the Method

The results of the quantitative branch detection were compared to the manually identified reference, i.e., the largest branch in each whorl. The quantitatively detected branches belonging to the same whorl were matched together with a corresponding reference branch based on their heights from the root collar. The minimum difference in height was used as the matching criteria, with a 15-cm threshold for the maximum difference between branches within same whorl. In other words, all the quantitatively detected branches that were within 15 cm of a certain manually identified branch were labeled as belonging to the same whorl. The 15-cm threshold was decided based on the visual inspections of the data and the matching results.

The detection method was analyzed for the detection accuracy using all whorls and in each sample tree separately. Whorl detection accuracy (%) was defined as follows:

$$\text{Accuracy}\,(\%) = \frac{n_a}{n_m + n_{fp}} * 100 \tag{4}$$

where n_a is the number of whorls detected correctly by the quantitative method, n_{fp} is the number of false positive detections made by the quantitative method, and n_m is the number of whorls identified visually. The whorl detection accuracy describes the methods ability to detect branches and to differentiate branches from other structures present in the point cloud. Additionally, the false positive rate was calculated as the ratio of n_{fp} to n_m.

The functionality of the quantitative branch detection method was assumed to be highly dependent of the point cloud density and completeness. Both parameters are in general strongly affected by the distance of the scanned object from the scanner. Therefore, the performance of the detection method was also compared against the whorl heights. Additionally, the lowest and highest detected whorls were compared to crown section limits H_{db} and H_{lc} as measured in the field (see Table II). This was done in order to reveal the possible self-occlusion caused by the tree crowns.

Branch diameter and insertion angle estimates derived from the RANSAC circle fitting method were compared to the reference measurements that included the branch diameters and insertion angles of the largest branch in each whorl derived from the manual circle fitting method. Using the matched whorls as described above, the maximum branch diameter and the insertion angle of that branch as measured by either method were compared within each whorl. The accuracies of the maximum branch diameter and the corresponding angle estimates in each whorl were evaluated in terms of bias and root-mean-squared error (RMSE)

$$\text{bias} = \frac{\sum_{t=1}^{n}(d_{m\,t} - d_{a\,t})}{n} \tag{5}$$

$$\text{RMSE} = \sqrt{\frac{\sum_{t=1}^{n}(d_{m\,t} - d_{a\,t})^2}{n}} \tag{6}$$

TABLE V
TREE-SPECIFIC ACCURACY OF THE QUANTITATIVE WHORL DETECTION METHOD

Whorl detection accuracy	Min	Mean	Max
Plot 1	50%	87.8%	100.0%
Plot 2	6.7%	44.4%	95.0%
Plot 3	44.4%	84.6%	100.0%
Plot 4	14.3%	60.8%	92.9%
Plot 5	33.3%	61.7%	85.7%
Plot 6	11.1%	64.1%	91.7%
Total	*6.7%*	*69.2%*	*100.0%*

The total number of reference whorls was 3403 and the number of trees 158.

where *t* gives the order of each measurement, d_m is the manually measured branch diameter or insertion angle of the largest branch in a whorl, d_a is the corresponding estimate derived from the quantitative method and *n* is $n_a - n_{fp}$. Both bias and RMSE were also calculated as percentages by dividing the results from (5) and (6) by the mean values of the reference measurements. The accuracy was inspected for the whole dataset and for each tree separately.

The abovementioned accuracies of whorl detection and the largest branch diameter and the corresponding branch angle estimates encompass the possibility that the largest branch in a whorl detected by the quantitative method is a different branch than that identified by visual inspection. This may be due to the quantitative method having not detected the same branch, or the diameter estimation, which is consistent with another branch in that whorl being larger. Therefore, we defined the sensitivity of the evaluation for the choice of branch, i.e., how much of the variation in the accuracy is due to the choice of branch within a whorl and how much to the branch modeling method. The largest branches identified manually were matched with the closest quantitatively measured branch within a 5-cm search radius in 3-D. The search radius was defined by the visual inspections of the data to ensure that the matched observations were from the same branch. The accuracy of the branch diameter and insertion angle estimation was defined for these branches as described above in (5) and (6).

IV. RESULTS

The quantitative whorl detection method detected correctly 2420 out of all 3403 (71.1%) manually identified whorls in the log-sections of the 158 trees. Considering also the number of false positives (64), the whorl detection accuracy was 69.9%. The ratio of false positives to the number of reference branches was 1.9%. The visual inspections indicated that the false positives were caused by loose bark, points left from surrounding tree crowns, stochastic noise, and a broken branch that was detected twice. In principle, the false detection rate can be understood as low. Three trees out of the 158 had no whorls detected by either the quantitative or the visual method within the log-section. Tree-specific accuracy statistics of the quantitative whorl detection for each plot are shown in Table V. The highest accuracy was achieved in plot 1, where the quantitative method had a minimum of 50%, mean 87.8%, and a maximum of 100% tree-specific whorl detection accuracy.

TABLE VI
TREE-SPECIFIC BIAS AND RMSE STATISTICS OF THE BRANCH DIAMETER AND INSERTION ANGLE ESTIMATES

	Bias						RMSE					
	Min	%	Mean	%	Max	%	Min	%	Mean	%	Max	%
Branch diameter (cm)												
Plot 1	-1.26	-62.1	0.28	7.2	1.61	40.6	0.22	11.1	1.89	62.1	4.38	171.3
Plot 2	-0.65	-23.3	0.19	6.6	1.32	45.3	0.01	0.3	2.33	77.0	9.09	304.6
Plot 3	-0.50	-15.2	0.30	9.3	1.02	27.0	0.32	11.6	1.64	54.9	4.63	141.5
Plot 4	-0.30	-12.1	0.35	10.5	1.17	30.6	0.00	0.0	1.96	62.1	3.83	154.0
Plot 5	-0.97	-32.9	0.45	12.8	1.36	34.7	0.15	4.9	1.91	58.0	5.27	178.8
Plot 6	-0.42	-14.7	0.30	8.4	1.71	34.4	0.35	12.5	1.99	62.1	9.40	189.7
Total	-1.26	-62.1	0.32	9.2	1.71	45.3	0.00	0.0	1.92	61.7	9.40	304.6
Branch insertion angle (°)												
Plot 1	-4.30	-6.0	4.14	6.2	11.94	18.4	8.09	13.9	19.16	28.9	34.00	50.2
Plot 2	-9.72	-16.5	-0.04	-0.3	8.52	13.8	1.97	2.9	16.05	25.1	33.85	57.7
Plot 3	-7.35	-11.7	0.68	0.6	19.44	28.0	7.42	11.2	14.76	22.9	31.92	53.4
Plot 4	-6.93	-12.8	1.08	1.5	13.50	21.4	4.69	7.6	16.35	25.3	29.50	46.8
Plot 5	-9.10	-17.1	-1.22	-2.1	15.79	21.1	9.22	15.6	15.98	25.3	29.11	42.2
Plot 6	-14.18	-22.1	-1.88	-3.0	4.07	6.0	3.06	4.9	12.98	19.6	20.40	29.9
Total	-14.18	-22.1	0.55	0.6	19.44	28.0	1.97	2.9	15.91	24.5	34.00	57.7

The number of whorls was 3403 and the number of trees 158.

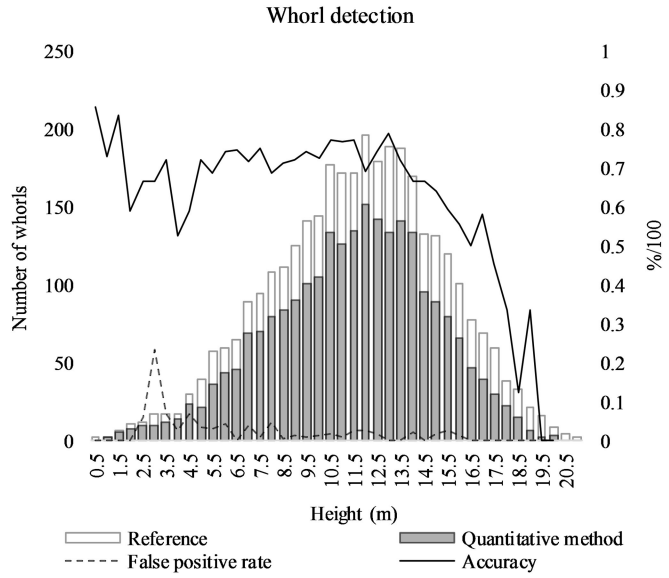

Fig. 3. White columns represent the distribution of the visually identified whorls in all 158 trees with respect to the whorl height. The gray columns represent the distribution of the quantitatively detected whorls with respect to the whorl height. The dashed black line shows the ratio of false positives to the number of manually detected whorls at given heights. The solid black line displays the whorl detection accuracy of the quantitative method at given heights.

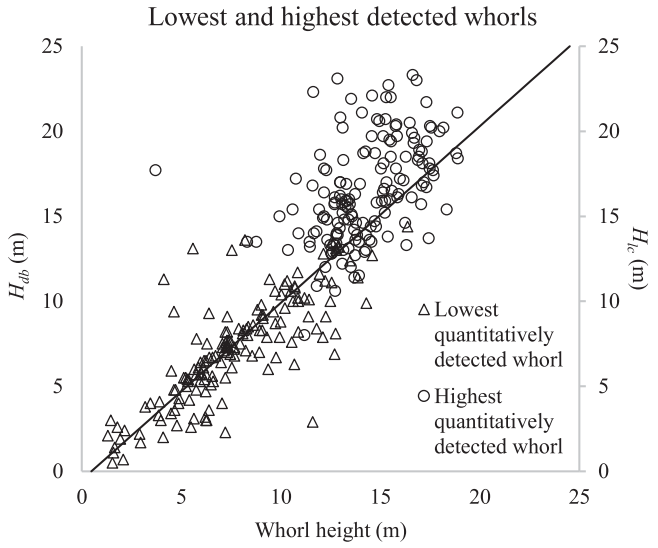

Fig. 4. Heights of the lowest whorls detected by the quantitative method (triangles) and the heights of the highest quantitatively detected whorls (circles) are plotted against the tree specific H_{db} on the left-hand and H_{lc} on the right-hand vertical-axes, respectively. The black diagonal line is the reference line. The number of trees was 158.

The functionality of the quantitative whorl detection method in respect to the heights of the detected whorls is visualized in Figs. 3 and 4. The distribution of the visually identified reference whorls along the length of the stem in Fig. 3 shows that the numbers of whorls that were visible in the point clouds was small in the lower parts of the trees, which was due to natural self-pruning, i.e., shedding of branches of Scots pine. The amount of manually identifiable whorls increased gradually and then decreased again higher in the trees. As illustrated in Fig. 4, the lowest quantitatively detected whorl's height in each tree correlated well with the H_{db} measured in the field for each tree (Pearson's correlation coefficient $r = 0.79$). Fig. 4 also shows that the highest quantitatively detected whorl tended to be lower than H_{lc}, which was due to the log limit (stem diameter >15 cm) being lower than H_{lc} for most trees. The highest detected whorl and H_{lc} showed correlation of $r = 0.44$.

In comparison to the manual reference measurements, the mean estimates of the maximum branch diameters and their insertion angle in the quantitatively detected whorls were underestimated by 0.34 cm (11.1%) and 0.68° (1.0%), and had RMSEs of 1.42 cm (46.0%) and 17.20° (26.3%), respectively. Descriptive statistics of tree-specific bias and RMSE of branch diameter and insertion angle estimates for each plot and in total are presented in Table VI. The estimation errors of the maximum branch diameter estimates and the corresponding insertion angles in the quantitatively detected whorls were evenly distributed with respect to the height from the root collar, i.e., the errors were not height dependent, as shown in Fig. 5.

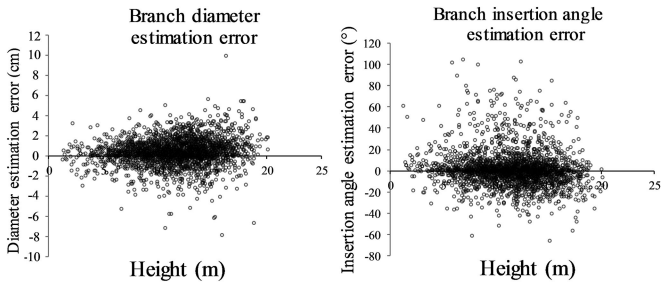

Fig. 5. Estimation error of the branch diameter (left) and insertion angle (right) of the largest branch in a whorl with respect to the height from the root collar for all branches. The number of whorls was 3403.

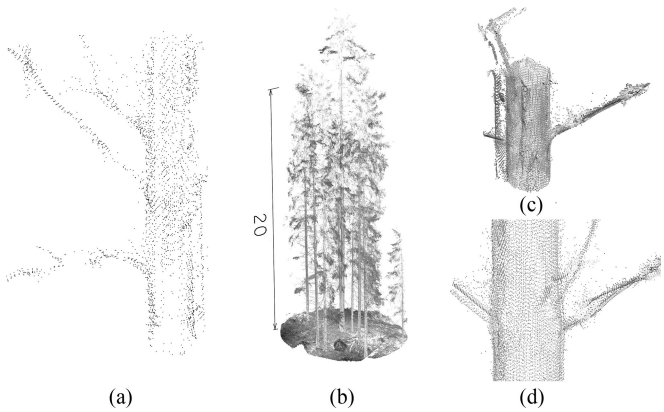

Fig. 6. Factors that adversely affect the whorl detection and branch modeling. (a) Branches at approximately 17-m height from the root collar, where the branch point cloud is sparse due to the increasing distance to the scanner and increasing self-occlusion effect. The branch shape is hardly represented in the point cloud data. (b) The tree in the middle: A sample tree on plot 4 situated amid heavily occlusive Norway spruces. (c) and (d): Wind distortion that causes the stem and branches appear multiplied and distorts their shape.

The abovementioned results include cases where the largest branch in a whorl detected by the quantitative method is a different branch than that in the reference data. The bias and RMSE of the branch diameter and insertion angle estimates were calculated separately for all branches that could be matched between the both datasets to assess the accuracy of the branch modeling procedure itself. The number of matched branches was 1658. The estimated diameter and insertion angles for matched branches had biases of 0.41 cm (12.6%) and 0.05° (0.0%), and RMSEs of 1.31 cm (40.4%) and 15.4° (23.4%), respectively.

Factors that affect the whorl detection and branch modeling are illustrated in Fig. 6: 1) Point clouds tend to be sparser toward the tree top, i.e., further from the scanner. Fig. 6(a) illustrates an example of sparse point cloud data at 17 m above the root collar. Under such a condition, the circular shape of the branch is not fully recorded, which makes the modeling of the branch extremely difficult, if not impossible. 2) The tree's own crown and that of the surrounding trees can cause considerable occlusion especially toward the tree tops. A heavy occlusion by surrounding Norway spruces is illustrated in Fig. 6(b). 3) Certain trees were heavily distorted due to the wind (see Table III), especially toward the tree tops (see Fig. 6(c) and (d)).

V. Discussion

Our study presented a quantitative branch detection and modeling method for multiscan TLS point clouds of individual Scots pine trees, including the first comprehensive evaluation of quantitatively derived branch parameters in a forest environment plot-, tree-, whorl-, and branch-specifically. The main motivation for the evaluation of the method was that the comparable state-of-the-art wood quality estimation systems currently used at sawmills that rely on X-ray scanning, provide information on whorl quantity and the maximum knot size within each whorl [8]. In the absence of X-ray equipment, the grading of logs is based on even sparser data on the knottiness, such as the size of the largest branch on a log surface [6]. Such grading approaches have been supported by Björklund and Petersson [33] who concluded in their study that the maximum knot diameter in a Scots pine saw-log is often a robust indicator of the overall knottiness of the log. The accuracy of similar wood quality indicators as currently used at sawmills' production and wood procurement was considered as a solid reference in assessing how useful and efficient quantitative TLS point cloud based branch structure data are for the estimation of wood quality in standing timber.

The stem detection and modeling method used in this study was originally introduced for stem detection and mapping in a forest environment [28]. However, in this study we extracted the sample trees manually in order to avoid the results of the quantitative branch detection and modeling being affected by the accuracy of tree extraction. Tree segmentation and extraction are separate topics that have been further treated in other studies, e.g., Zhong *et al*. [34], Raumonen *et al*. [23], and Xia *et al*. [35]. Such methods are thus readily available to separate the individual trees for further analyses, including the current study. All the stem and branch detection and modeling parts of the quantitative method presented in this study are point-processing techniques that utilize 3-D-coordinates of individual points, and require no further information such as intensity values. However, should multi- or hyperspectral TLS or any other more advanced point-cloud-producing techniques become more commonly available in the future, implementing additional information could further improve the proposed method. Such improvements could include distinguishing between dead and live branches, which is of high importance in the grading of sawn goods [3].

The quantitative method found the majority of the whorls in most trees (see Table V) compared to the actual number found by manual identification. As the functionality of the method was dependent mainly on the density and completeness of the point cloud and the spatial accuracy of the points, three factors prevalent in the forest environment of the present study were found to affect the whorl detection accuracy, namely: Distance from the scanner, occlusion, and wind. First, Fig. 3 illustrates a rapid decrease in the number of visually detectable whorls as the distance from the scanner increases. More importantly, the share of quantitatively detected whorls decreases even more rapidly. Second, the scanning setup was carefully planned beforehand in order to minimize the occlusion, but the occlusion effect cannot completely be avoided (see Fig. 6(b)). The growing stock

volume in plot 4 was 400 m^3/ ha (see Table I) and is likely to have affected the detection accuracy on that plot (see Table V). Self-occlusion caused by tree's own crown is also difficult to overcome, as it requires balancing between visibility and distance from the scanner. The scope of this study was limited to the log section and H_{lc} was in many trees above the log section (see Fig. 4), e.g., on plots 4 and 5 (see Table II); thus, the self-occlusion effect on these plots may not have been a major source of inaccuracy in branch detection. Third, the time for data collection was limited due to the harvesting schedule. For that reason, the data were collected regardless of the presence or absence of windy conditions on certain dates. However, this situation mirrors what can be expected under practical working conditions. Plot 2 had the lowest whorl detection accuracy among the six plots studied (see Table V), which was at least partly due to a combination of high H_{db} (see Table II) in the sample trees and the consequently low point density on branches (see Table III), and the strong wind (see Table III).

The factors that were found to affect the method's functionality are supported by previous findings, which reported that TLS-based modeling of the tree structure is sensitive to surrounding conditions [10], [25], [26]. How increasing the point cloud density or decreasing the distance of the scanning positions to targeted trees would affect the whorl detection and branch modeling accuracy should further be tested. However, it is also worth noting that the TLS point cloud data used in this study represent the best terrestrial point cloud quality in terms of point density currently available for forest conditions. The scanning setup in this study, i.e., five to ten scans for every three to six trees already resulted in high point densities that are most likely not achievable for practical applications with reasonable cost efficiency. On the other hand, it is also possible to achieve a similar point density as that obtained in this study using MLS [15], which would involve a scanner mounted on a harvester. Data acquisition with MLS has been reported to be faster than with TLS [10].

The scope of this study allowed the method to be evaluated for the accuracy of the maximum branch diameter in each whorl, regardless of which exact branch was in question. The results showed that even though the branch diameter and insertion angle estimation errors had variation, there was little bias and the errors were not height dependent (see Fig. 5 and Table VI). However, erroneous branch parameter estimates may cause over- or underestimation of the internal knot size and, consequently, the expected wood quality. Therefore, we also tested the accuracy of the branch modeling method itself by evaluating the accuracy of the branch diameter and insertion angle using individual branches that were matched based on their 3-D location. The results showed only a slightly better RMSE in comparison to the whorl-specific accuracies, and a slightly larger bias. The results imply that the choice of branch within a whorl may not play any major role in the estimation of the whorl-specific branch parameters.

The accuracy of TLS point cloud based tree models for estimating individual branch diameters using circle fitting has not been evaluated until now. Despite the lack of directly comparable branch modeling studies, it is worth noting that fitting circles to branches is similar to fitting circles to stems in a single-scan mode as only a half of a circular object is visible. Olofsson *et al*. [36] used a similar RANSAC circle fitting approach as that used in this study and they applied this to give a DBH estimation in a single-scan point cloud. They reported RMSEs in the range of 2.6−5.9 cm (9.6−21.4%) in the DBH estimation, the errors increased as the distance from the scanner increased. Additionally, Koreň *et al*. [37] compared several different circle fitting methods for their DBH estimation, and reported RMSEs of 1.71−12.49 cm when using the single-scan setup. In the current study, the RMSEs of branch diameters were similar in terms of absolute values (see Table VI). However, the relative errors (RMSE-%) were clearly higher due to branches being smaller than the stems. Similar to that reported by Olofsson *et al*. [36], this present study found the errors increased further from the scanner, i.e., toward the tree tops (see Fig. 5).

The matching errors in coregistering of the multiple scans presented in Table III might also have had a small effect on the accuracy of the branch detection and branch parameter estimates. The effect of wind and the registration errors could at least partly be overcome by processing the point clouds separately, instead of as a merged multiscan point cloud [11], [26], [38]. Moreover, an approach such as presented by Côté *et al*. [24] that would combine TLS point cloud based tree models with a branch growth model, could allow estimation of the branching structure and branch parameters also in the occluded parts of the tree.

Pyörälä *et al*. [39] used TLS point cloud based manual branch measurements and compared them to whorl data obtained by X-ray scanning. In that study, 55% of the whorl structure within the log sections that was detected by the X-ray method was also detected using the TLS method. The manual branch diameter measurements obtained from the TLS point clouds were for the most part found to be inconsistent with internal knot diameters measured by means of X-ray scanning. However, the difference between the tree-specific maximum knot and branch diameters was not statistically significant. The results of the previous and the current study indicate that it is possible that some relationship between the TLS point cloud based quantitative branch diameter estimates and the expected wood quality could be established, if the largest knot in a log was considered to be a sufficient indicator of wood quality as was reported by Björklund and Petersson [33]. In addition, the lowest quantitatively detected whorl correlated well with H_{db} (see Fig. 4), a variable that has been previously used for wood quality estimations [40], [41].

VI. Conclusion

A TLS point cloud based method to model the main branching structure of a tree, i.e., branch bases that divert from the stem method was tested on 158 mature Scots pine trees that had grown on 6 forest plots and the whorls were quantitatively detected with an accuracy of 69.9%. The whorl detection accuracy decreased toward the tree tops, which demonstrated the effect of the point density on the method's functionality. The results suggest that when developing the use of TLS-based compre-

hensive tree models and quantitative methods for measurement of wood quality indicators, the quality and point density of the point cloud data can affect the results. These factors should therefore be addressed in the studies in addition to the algorithm development.

ACKNOWLEDGMENT

The authors would like to thank Evo Forest School for providing their forest plots and facilities to our use. They would also like to thank J. Uusitalo, O. Ylhäisi, and P. Helminen from Natural Resources Institute Finland for collecting and providing the field data. The language was edited by A. Mclean (Ph.D.).

REFERENCES

[1] H. Korpunen, S. Mochan, and J. Uusitalo, "An Activity-Based costing method for sawmilling," *Forest Products J.*, vol. 60, no. 5, pp. 420–431, Aug. 2010.

[2] D. Sandberg, "Distortion and visible crack formation in green and seasoned timber: Influence of annual ring orientation in the cross section," *Holz Als Roh-Und Werkstoff*, vol. 63, no. 1, pp. 11–18, Feb. 2005.

[3] "Grading rules for Pine (Pinus Sylvestris) and Spruce (Picea Abies) Sawn Timber," 2016.

[4] J. Benjamin, Y. Chui, and S. Zhang, "A method to assess lumber grade recovery improvement potential for black spruce logs based on branchiness," *Forest Products J.*, vol. 57, no. 12, pp. 34–41, 2007.

[5] M. Samson, "Modeling of knots in logs," *Wood Sci. Technol.*, vol. 27, no. 6, pp. 429–437, 1993.

[6] C. L. Todoroki, R. A. Monserud, and D. L. Parry, "Predicting internal lumber grade from log surface knots: Actual and simulated results," *Forest Products J.*, vol. 55, no. 6, pp. 38–47, Jun. 2005.

[7] U. Nordmark and J. Oja, "Prediction of board values in Pinus sylvestris sawlogs using x-ray scanning and optical three-dimensional scanning of stems," *Scand. J. Forest Res.*, vol. 19, no. 5, pp. 473–480, Oct. 2004.

[8] J. Oja, S. Grundberg, J. Fredriksson, and P. Berg, "Automatic grading of sawlogs: A comparison between X-ray scanning, optical three-dimensional scanning and combinations of both methods," *Scand. J.Forest Res.*, vol. 19, no. 1, pp. 89–95, 2004.

[9] A. Kangas, H. Hurttala, H. Mäkinen, and J. Lappi, "Estimating the value of wood quality information in constrained optimization," *Can. J.Forest Res.*, vol. 42, no. 7, pp. 1347–1358, 2012.

[10] X. Liang *et al.*, "Terrestrial laser scanning in forest inventories," *ISPRS J. Photogramm. Remote Sens.*, vol. 115, pp. 63–77, 2016.

[11] N. Saarinen *et al.*, "Feasibility of Terrestrial laser scanning for collecting stem volume information from single trees," *ISPRS J. Photogramm. Remote Sens.*, vol. 123, pp. 140–158, 2017.

[12] M. Abegg, D. Kükenbrink, J. Zell, M. E. Schaepman, and F. Morsdorf, "Terrestrial laser scanning for forest Inventories—Tree diameter distribution and scanner location impact on occlusion," *Forests*, vol. 8, no. 6, p. 184, 2017. [Online]. Available: http://www.mdpi.com/about/announcements/784

[13] J. E. Luther *et al.*, "Predicting wood quantity and quality attributes of balsam fir and black spruce using airborne laser scanner data," *Forestry*, vol. 87,2013, Art. no. cpt039.

[14] M. Vastaranta *et al.*, "Multisource Single-Tree inventory in the prediction of tree quality variables and logging recoveries," *Remote Sens.*, vol. 6, no. 4, pp. 3475–3491, Apr. 2014.

[15] X. Liang, J. Hyyppä, A. Kukko, H. Kaartinen, A. Jaakkola, and X. Yu, "The use of a mobile laser scanning system for mapping large forest plots," *IEEE Geosci. Remote Sens. Lett.*, vol. 11, no. 9, pp. 1504–1508, Sep. 2014.

[16] Z.-L. Cheng, X.-P. Zhang, and B.-Q. Chen, "Simple reconstruction of tree branches from a single range image," *J. Comput. Sci. Technol.*, vol. 22, no. 6, pp. 846–858, 2007.

[17] B. Gorte and N. Pfeifer, "Structuring laser-scanned trees using 3D mathematical morphology," *Int. Arch. Photogramm. Remote Sens.*, vol. 35, no. B5, pp. 929–933, 2004.

[18] A. Bucksch and R. Lindenbergh, "CAMPINO—A skeletonization method for point cloud processing," *ISPRS J. Photogramm. Remote Sens.*, vol. 63, no. 1, pp. 115–127, 2008.

[19] J.-F. Côté, J.-L. Widlowski, R. A. Fournier, and M. M. Verstraete, "The structural and radiative consistency of three-dimensional tree reconstructions from terrestrial lidar," *Remote Sens. Environ.*, vol. 113, no. 5, pp. 1067–1081, 2009.

[20] P. Raumonen *et al.*, "Fast automatic precision tree models from terrestrial laser scanner data," *Remote Sens.*, vol. 5, no. 2, pp. 491–520, 2013.

[21] F. Boudon *et al.*, "Quantitative assessment of automatic reconstructions of branching systems obtained from laser scanning," *Ann. Bot.*, vol. 114, no. 4, pp. 853–862, 2014.

[22] E. Bournez, T. Landes, M. Saudreau, P. Kastendeuch, and G. Najjar, "From TLS point clouds to 3-D models of trees: A comparison of existing algorithms for 3-D tree reconstruction," *Int. Arch. Photogramm., Remote Sens. Spatial Inf. Sci.*, vol. 42, pp. 113–120, 2017.

[23] P. Raumonen, E. Casella, K. Calders, S. Murphy, M. Åkerblom, and M. Kaasalainen, "Massive-scale tree modelling from TLS data," *ISPRS Ann. Photogramm., Remote Sens. Spatial Inf. Sci.*, vol. 2, no. 3, pp. 189–196, 2015.

[24] J.-F. Côté, R. A. Fournier, and J. E. Luther, "Validation of L-architect model for balsam fir and black spruce trees with structural measurements," *Can. J. Remote Sens.*, vol. 39, no. 1, pp. 41–59, 2013.

[25] M. Dassot, A. Colin, P. Santenoise, M. Fournier, and T. Constant, "Terrestrial laser scanning for measuring the solid wood volume, including branches, of adult standing trees in the forest environment," *Comput. Electron. Agriculture*, vol. 89, pp. 86–93, 2012.

[26] L. Eysn, N. Pfeifer, C. Ressl, M. Hollaus, A. Grafl, and F. Morsdorf, "A practical approach for extracting tree models in forest environments based on equirectangular projections of terrestrial laser scans," *Remote Sens.*, vol. 5, no. 11, pp. 5424–5448, 2013.

[27] D. Bayer, S. Seifert, and H. Pretzsch, "Structural crown properties of Norway spruce (Picea abies [L.] Karst.) and European beech (Fagus sylvatica [L.]) in mixed versus pure stands revealed by terrestrial laser scanning," *Trees*, vol. 27, no. 4, pp. 1035–1047, 2013.

[28] X. L. Liang, P. Litkey, J. Hyyppä, H. Kaartinen, M. Vastaranta, and M. Holopainen, "Automatic stem mapping using single-scan terrestrial laser scanning," *IEEE Trans. Geosci. Remote Sens.*, vol. 50, no. 2, pp. 661–670, Feb. 2012.

[29] M. Vaaja, J.-P. Virtanen, M. Kurkela, V. Lehtola, J. Hyyppä, and H. Hyyppä, "The effect of wind on tree STEM parameter estimation using terrestrial laser scanning," *ISPRS Ann. Photogramm., Remote Sens. Spatial Inf. Sci.*, vol. III-8, pp. 117–122, 2016.

[30] J. W. Cooley and J. W. Tukey, "An algorithm for the machine calculation of complex Fourier series," *Math. Comput.*, vol. 19, no. 90, pp. 297–301, 1965.

[31] P. Du, W. A. Kibbe, and S. M. Lin, "Improved peak detection in mass spectrum by incorporating continuous wavelet transform-based pattern matching," *Bioinformatics*, vol. 22, no. 17, pp. 2059–2065, 2006.

[32] M. A. Fischler and R. C. Bolles, "Random sample consensus: a paradigm for model fitting with applications to image analysis and automated cartography," *Commun. ACM*, vol. 24, no. 6, pp. 381–395, 1981.

[33] L. Björklund and H. Petersson, "Predicting knot diameter of Pinus sylvestris in Sweden," *Scand. J. Forest Res.*, vol. 14, no. 4, pp. 376–384, 1999.

[34] L. Zhong, L. Cheng, H. Xu, Y. Wu, Y. Chen, and M. Li, "Segmentation of individual trees from TLS and MLS data," *IEEE J. Sel. Topics Appl. Earth Observ. Remote Sens.*, vol. 10, no. 2, pp. 774–787, Feb. 2017.

[35] S. Xia, C. Wang, F. Pan, X. Xi, H. Zeng, and H. Liu, "Detecting stems in dense and homogeneous forest using single-scan TLS," *Forests*, vol. 6, no. 11, pp. 3923–3945, 2015.

[36] K. Olofsson, J. Holmgren, and H. Olsson, "Tree stem and height measurements using terrestrial laser scanning and the ransac algorithm," *Remote Sens.*, vol. 6, no. 5, pp. 4323–4344, 2014.

[37] M. Koreň, M. Mokroš, and T. Bucha, "Accuracy of tree diameter estimation from terrestrial laser scanning by circle-fitting methods," *Int. J. Appl. Earth Observ. Geoinform.*, vol. 63, pp. 122–128, 2017.

[38] X. L. Liang and J. Hyyppä, "Automatic stem mapping by merging several terrestrial laser scans at the feature and decision levels," *Sensors*, vol. 13, no. 2, pp. 1614–1634, 2013.

[39] J. Pyörälä *et al.*, "Comparison of terrestrial laser scanning and X-ray scanning in measuring Scots pine (Pinus sylvestris L.) branch structure," *Scand. J. Forest Res.*, vol. 33, no. 3, pp. 291–298, 2017.

[40] J. Uusitalo, "Preharvest measurement of pine stands for sawing production planning," *Acta Forestalia Fennica*, vol. 259, pp. 1–56, 1997.

[41] H. T. Lyhykäinen, H. Mäkinen, A. Mäkelä, S. Pastila, A. Heikkilä, and A. Usenius, "Predicting lumber grade and by-product yields for Scots pine trees," *Forest Ecology Manage.*, vol. 258, no. 2, pp. 146–158, Jun. 15 2009.

Jiri Pyörälä received the M.Sc. degree from the University of Helsinki, Helsinki, Finland, in forest resource science and technology with a specialization in wood technology in 2014. He is currently working toward the Ph.D. degree at the University of Helsinki.

He is currently a Researcher with the Centre of Excellence in Laser Scanning Research and the Finnish Geospatial Research Institute. His research interests include wood and timber properties, with a special interest on the use of laser scanning technology to assess the standing timber wood quality.

Xinlian Liang received the Doctoral degree in geoinformatics from Aalto University, Espoo, Finland, in 2013.

He is a Research Manager and the Group Leader of the Forest Digitization with the Department of Remote Sensing and Photogrammetry, Finnish Geospatial Research Institute, and with the Centre of Excellence in Laser Scanning Research, Academy of Finland. His current research interests include the innovative geospatial solutions in modeling forest ecosystem, from all kinds of point clouds as well as imagery technologies.

Mikko Vastaranta received the M.Sc. and Ph.D. degrees in forest resource science and technology from the University of Helsinki (UH), Helsinki, Finland, in 2007 and 2012, respectively.

During the last five years, he worked as a Research Scientist with the Centre of Excellence in Laser Scanning Research, University Lecturer in Forest Planning with UH, and a Visiting Research Scientist with Pacific Forestry Centre, (Canadian Forestry Service, Natural Resources Canada). He is currently an Associate Professor with the School of Forest Sciences, University of Eastern Finland. He also holds an Adjunct Professorship of remote sensing of forests, UH. He has authored or co-authored more than 100 peer-reviewed scientific articles. His current research interests include detailed remote sensing of forests and improved use of forest resource information.

Ninni Saarinen received M.A. degree in education from the University of Helsinki, in 2014, and the Ph.D. degree in agriculture and forestry from University of Helsinki, in 2016, three years after starting her research career. She is a Postdoctoral Researcher with the Department of Forest Sciences, University of Helsinki, Helsinki, Finland, and with the Centre of Excellence in Laser Scanning Research. She is currently a Visiting Researcher with the School of Forest Sciences, University of Eastern Finland. She has also been working as a Visiting Research Scientist with Pacific Forestry Centre, Victoria, BC, Canada(Canadian Forest Service, Natural Resources Canada). Her current research interests include detailed characterization and modeling of forest ecosystems as well as utilization of time series in forest monitoring at various levels.

Ville Kankare born in 1985. He received the M.Sc. degree in forest resource science and technology in December 2010 and the Ph.D. degree in agriculture and forestry in August 2015, both from the Department of Forest sciences, University of Helsinki (UH), Helsinki, Finland.

He is currently a Postdoctoral Researcher under Prof. M. Holopainen's research group at the UH, and with the Center of Excellence in Laser scanning research. He has authored or co-authored more than 50 peer-reviewed articles. His current research interests include precision forestry through 3-D remote sensing.

Yunsheng Wang received the Doctoral degree in natural sciences from the University of Freiburg, Breisgau, Germany, in 2008.

From 2010 to 2012, she was a Project Manager in Environmental Management and Climate Change at the Deutsche Gesellschaft für Internationale Zusammenarbeit (GIZ) GmbH. She is currently a Senior Research Scientist with the Centre of Excellence in Laser Scanning Research, Academy of Finland, Helsinki, Finland, and with the Finnish Geospatial Research Institute, Masala, Finland. Her main research interests include the assessment of ecosystem services and 3-D modeling from point cloud data.

Markus Holopainen received the M.Sc. and Ph.D. degrees in forestry from the University of Helsinki (UH), Helsinki, Finland, in 1993 and 1998, respectively, and the M.Sc. and Dr. Tech. degrees from the Department of Surveying, Aalto University (AU), Espoo, Finland, in 1995 and 2011, respectively.

Since 2012, he has been a Professor of geoinformatics with the Departments of Forest Sciences, Forest Resource Management, and Geoinformatics, University of Helsinki.

He is the Head of the Candidate Degree program in Forest Sciences at the University of Helsinki and the Vice-Director in the Centre of Excellence in Laser Scanning Research. He has authored and co-authored 240+ publications of which 140+ are published in peer-reviewed scientific journals or books. His current research interests include utilization of 3-D/4-D data in forest mapping, inventory, management, monitoring, and precision forestry. Since 2014, his research group in the Laboratory of Forest Resource Management and Geo-Information Science (Forest-GIS-Lab) (http://blogs.helsinki.fi/4d-gis/) has been a part of the Centre of Excellence in Laser Scanning Research CoE-LaSR (http://laserscanning.fi/).

Juha Hyyppä received the M.Sc., Dr.Ing., and Dr.Sc. degrees, all with honors, from Helsinki University of Technology, Espoo, Finland, in 1987, 1990, and 1994, respectively.

He is currently a Professor of remote sensing and photogrammetry with Finnish Geospatial Research Institute, the Director of the Centre of Excellence in Laser Scanning Research, laserscanning.fi, and a Distinguished Professor with Shinshu University (Japan). His references include 30-years experience in research team leadership, coordination of 10+ international science projects, and author of 180+ ISI Web of Science listed papers. His research interests include laser scanning systems, their performance and new applications, especially related to mobile, personal, and ubiquitous laser scanning and their point cloud processing especially to forest information extraction.